

Title:

The correlation of indentation size effect experiments with pyramidal and spherical indenters

Author(s):

J. G. Swadener, E. P. George and G. M. Pharr

Submitted to:

<http://lib-www.lanl.gov/la-pubs/00796515.pdf>

The correlation of indentation size effect experiments with pyramidal and spherical indenters

J. G. Swadener¹, E. P. George² and G. M. Pharr^{2,3}

¹ Los Alamos National Laboratory, MST-8 MS-G755, Los Alamos, NM 87545 USA

² Metals and Ceramics Division, Oak Ridge National Laboratory, Oak Ridge, TN 37831 USA

³ Department of Materials Science and Engineering, University of Tennessee, Knoxville, TN 37996 USA

ABSTRACT

Experiments were conducted in annealed iridium using pyramidal and spherical indenters over a wide range of load. For a Berkovich pyramidal indenter, the hardness increased with decreasing depth of penetration. However, for spherical indenters, hardness increased with decreasing sphere radius. Based on the number of geometrically necessary dislocations generated during indentation, a theory that takes into account the work hardening differences between pyramidal and spherical indenters is developed to correlate the indentation size effects measured with the two indenters. The experimental results verify the theoretical correlation.

INTRODUCTION

Numerous indentation experiments over the last sixty years have shown that the hardness of crystalline materials measured by a pyramidal indenter increases with decreasing depth for small indents, which is known as the indentation size effect. Much of the early work has been reviewed by Mott [1]. Recent nanoindentation [2-4] studies have shown even greater increases in hardness for depths less than 1 μm .

Ashby [5] proposed that indentation with a flat punch would produce geometrically necessary dislocations [6], which would lead to an increase in hardness. Nix and Gao [7] adapted Ashby's concept to describe the geometrically necessary dislocations produced by a conical or pyramidal indenter. They incorporated Taylor hardening to develop a model that predicted an increase in hardness with decreasing depth in agreement with earlier nanoindentation experiments. More recent studies have shown only limited agreement with the Nix and Gao model [8-9]. It can be shown that this disagreement is due in part to the way in which the model accounts for the work hardening that occurs during indentation.

Spherical indentation results are presented that do not show a size effect due to penetration depth, but rather a size effect based on the radius of the sphere. In addition, spherical indentation can be used to decouple work hardening and indentation size effects. Based on the concept of geometrically necessary dislocations, a relation is developed to correlate the size effects measured with spherical and pyramidal indenters.

THEORY

A summary of the Nix and Gao model is given first followed by an extension to spherical indenters. The theory is presented in brief with details and extensions to other geometries to be published separately [10]. The models assume the generation of geometrically necessary dislocations below the indent as shown schematically in Fig. 1. The Nix and Gao [7] model for a conical indenter estimates the density of geometrically necessary dislocations (ρ_G) as:

$$\rho_G = 3 \tan^2 \theta / 2bh, \quad (1)$$

where $\tan\theta$ is the slope of the cone surface, b is the dislocation Burgers vector and h is the depth of the indent. The model employs Taylor hardening, given by $\tau = \alpha\mu b(\rho_G + \rho_S)^{1/2}$, the von Mises yield criterion, given by $\sigma = \tau\sqrt{3}$, and the Tabor relation between hardness (H) and flow stress (σ) given by $H = 3\sigma$, where τ is the shear stress, α is the shape factor in the Taylor model (usually close to 0.5), μ is the shear modulus, and ρ_S is the density of statistically stored dislocations. Using the above relations, the Nix and Gao model predicts the following relation for hardness as a function of indentation depth:

$$H = H_0(1 + h^*/h)^{1/2}, \quad (2)$$

where $H_0 = 3\alpha\mu b(3\rho_S)^{1/2}$ and the length scale $h^* = 3 \tan^2 \theta / 2b\rho_S$. Arsenlis and Parks [11] showed that, due to crystallographic considerations, the actual number of dislocations produced is generally greater than the number of geometrically necessary dislocations by a factor of \acute{r} , which they called the Nye factor. This can be incorporated into the Nix and Gao model by multiplying ρ_G by \acute{r} in the above derivation, which results in Eq. (2) if the length scale is redefined as: $h^* = 3\acute{r}\tan^2 \theta / 2b\rho_S$. Experimental results [2-4, 7-9] indicate that h^* can vary from 0.5 to 50 μm .

Following a similar procedure, it can be shown that the geometrically necessary dislocation density for a spherical indenter is:

$$\rho_G = 1/bR, \quad (3)$$

where R is the spherical radius of the indent (see Fig. 1b). This leads to the prediction that hardness measured by spherical indenters does not show a similar depth dependence, but instead, shows a dependence based on the spherical radius of the indent, which is given as:

$$H = H_0(1 + R^*/R)^{1/2}, \quad (4)$$

where H_0 is the same as above and $R^* = \acute{r}/b\rho_S$, which is a length scale comprised only of material properties. Note that the length scales for conical and spherical indenters can be related as $h^* = 3R^* \tan^2 \theta / 2$.

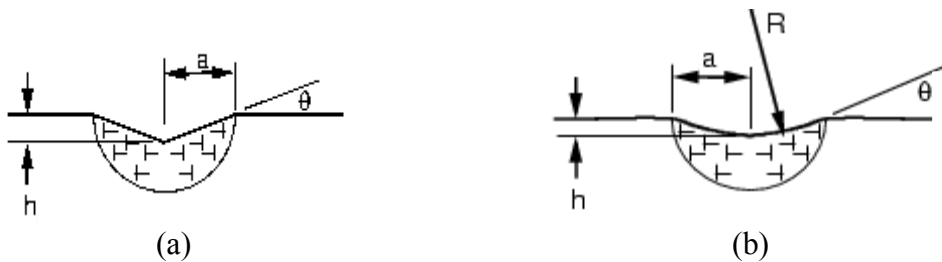


Figure 1. Models for geometrically necessary dislocations: (a) conical indenter (after Nix and Gao [7]) and (b) spherical indenter.

EXPERIMENTAL DETAILS

Nanoindentation experiments were conducted at 23°C using spherical and Berkovich (three sided pyramid) indenters. Displacements and loads were measured with a resolution of 0.16 nm and 0.3 μN , respectively. The material examined was a 0.5 mm thick specimen of iridium alloyed with 0.3 pct W and 60 ppm Th. The specimen was recrystallized for 1 hr at 1300°C, which resulted in a grain size of approximately 30 μm . For nanoindentation with a diamond Berkovich tip, the continuous stiffness measurement mode was used, and the tip shape was calibrated by conducting experiments on a fused quartz standard [13]. Data were analyzed using the Oliver and Pharr [13] method. Additional hardness tests were conducted using a Berkovich tip at loads of 25 to 1000g in a microhardness tester and at a load of 15 kg in a Rockwell hardness tester. The microhardness indent areas were measured with a video microscope system, which had a 0.25 μm resolution. For spherical indenters, the contact radius (a) was determined using the geometry of the sphere, the measured maximum and final depths and the formula developed by Field and Swain [14]. Additional experimental details are published elsewhere [10].

RESULTS AND DISCUSSION

Hardness values obtained with a Berkovich indenter were determined from continuous stiffness measurements using the Oliver and Pharr [13] method for data ranging from depths of 30 nm to 1.8 μm and for maximum loads up to 300 mN. Following the method proposed by Nix and Gao (1998), the hardness results obtained from nanoindentation, microindentation and the Rockwell hardness tester fitted with a Berkovich tip are plotted in Fig. 2 as $(H/H_0)^2$ versus $1/h$. A value of $H_0 = 2.5$ GPa, corresponding to the measured hardness at the greatest depth tested (50 μm), was used for this plot. Over the range where microhardness and nanohardness results overlap, there is close agreement. At depths less than 50 nm, rounding of the indenter tip influences the hardness measurement. Therefore, we restrict our discussion to depths greater than 50 nm. The Nix and Gao model prediction for $H_0 = 2.5$ GPa and $h^* = 2.6$ μm is also shown in Fig. 2 for comparison. The prediction agrees with the microhardness data within one standard deviation, but diverges significantly from the nanohardness results for $h < 1$ μm .

The hardness for the 5 spherical indenters used in this study is plotted versus a/R in Fig. 3. The effective strain as defined by Tabor ($0.2a/R$) [12] is indicated on the upper ordinate in Fig. 3. For $a/R < 0.03$, the hardness increases rapidly due to the transition from elastic dominated to plastic dominated deformation [12]. For $a/R > 0.03$, the hardness measured by each sphere increases at a rate approximately parallel to three times the flow stress (s_f), which is also plotted versus effective strain as shown in Fig. 3. The flow stress was determined from uniaxial tension tests, in which the material exhibited linear work hardening.

The data shown in Fig. 3 points out the chief advantage of using spherical indentation: since the size effect for a spherical indenter is not related to the depth of penetration, the effects of work hardening can be de-coupled from the indentation size effect. Work hardening effects are seen for each sphere as the linear increase in hardness with increasing a/R , while the different hardness values for different spheres at the same value of a/R illustrate the indentation size effect.

Because of the effects of work hardening, comparison of the hardness results for the different spheres must be done at the same effective strain and thus the same a/R value, which requires

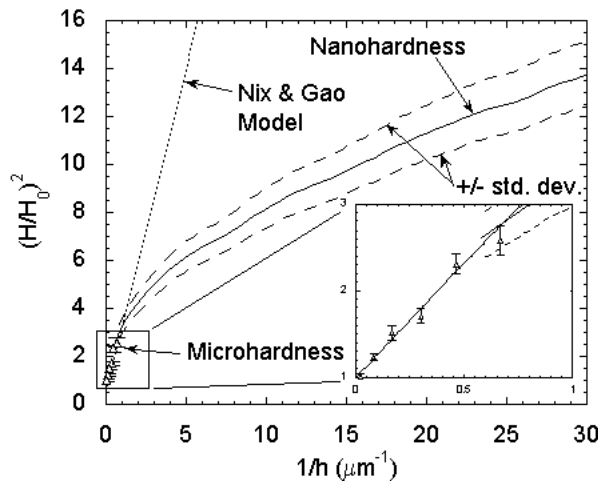


Figure 2. Indentation size effect in annealed iridium measured with a Berkovich indenter (Δ and solid line) and comparison of experiments with the Nix and Gao (1998) model for $H_0 = 2.5$ GPa and $h^* = 2.6 \mu\text{m}$ (dotted line).

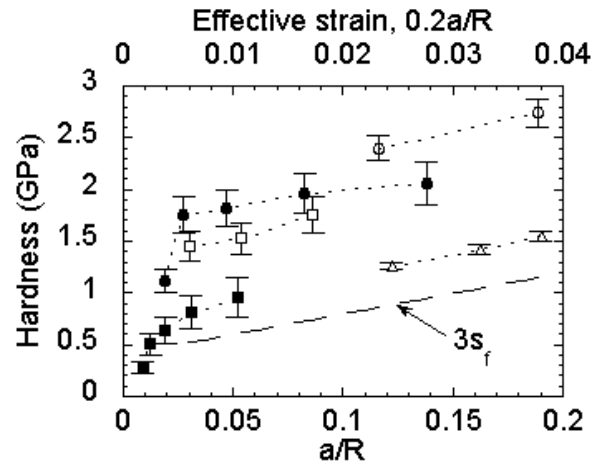


Figure 3. Variation of hardness in annealed iridium with a/R for spherical indenters: comparison of experiments ($R = 14 \mu\text{m}$, \circ ; $R = 69 \mu\text{m}$, \bullet ; $R = 122 \mu\text{m}$, \square ; $R = 318 \mu\text{m}$, \blacksquare ; $R = 1600 \mu\text{m}$, Δ) and $3s_f$.

extrapolation of some of the data. The data for the $14 \mu\text{m}$ and $1600 \mu\text{m}$ spherical tips were extrapolated parallel to the tensile work hardening curve to $a/R = 0.05$, which is within the fully plastic regime but where the effects of work hardening are small. The hardness for $a/R = 0.05$ (1% effective strain) for the five spherical tips is shown in Fig. 4. For the $1600 \mu\text{m}$ sphere, R was estimated to be 10 % greater than the radius of the indenter (R_s). For the other spheres, R was determined from the measured maximum and final depths. The average hardness is approximately the same for the largest two spheres, but increases monotonically with decreasing R for the other indenters. Since, within experimental uncertainty, the hardness measured by the two largest spheres does not increase, this value of hardness is indicated as the macroscopic hardness ($H_0 = 0.9$ GPa). The parameters $H_0 = 0.9$ GPa and $R^* = 250 \mu\text{m}$ provide a good fit to the data for large spheres. For these values of H_0 and R^* and $\dot{\epsilon} = 2$, the value of α is determined from the definition of H_0 and R^* as 0.52, which is within the range expected for α for FCC metals [15]. The hardness predicted by Eq. 4 agrees reasonably well with the experimental results for $R > 80 \mu\text{m}$, but diverges for smaller values of R . Spherical indentation studies are often conducted with spherical radii as small as $1 \mu\text{m}$, but length scale effects are often overlooked. These results point out that length scale effects must be considered when interpreting indentation results obtained with small spheres.

For pyramidal indenters, Nix and Gao [7] followed the traditional approach [5] of including dislocations produced by work hardening in the statistically stored dislocation density (ρ_s). In their procedure, H_0 is determined from the macroscopic hardness, that is, the hardness determined when $h \gg h^*$. For a Berkovich or Vickers indenter, the effective strain that occurs during indentation is 7% [12]. The macroscopic hardness of 2.1 GPa measured with a Berkovich tip has a sizable component due to work hardening compared to the largest spheres. However, the spherical indentation results show that the indentation size effect is completely separate from the work hardening that occurs during indentation (the increase in hardness with increasing effective strain). Therefore, we propose that the dislocations produced by work hardening during

indentation not be included in ρ_s , that H_0 correspond to a macroscopic hardness without work hardening, and that the work hardening component be added separately. Motivated by the spherical indentation results, we find that an effective strain of 1% gives an accurate value for H_0 in annealed FCC metals. Following the proposed method, Eq. (2) is modified as:

$$H = H_0(1 + h^*/h)^{1/2} + H_I, \quad (5)$$

where H_0 is based on the hardness measured at an effective strain of 1% and H_I is a work hardening component representing the increase in hardness from an effective strain of 1% to an effective strain of $\varepsilon = 0.2 \tan \theta$. Eq. (5) was found to give better agreement with combined spherical and pyramidal indentation data than Eq. (2) for the two cases studied.

Based on the observed work hardening in tensile test results, the expected difference between hardness values determined at 1% and 7% effective strain values for our iridium specimens is $H_I = 1.2$ GPa. Decreasing the hardness determined by a Berkovich indenter that was shown in Fig. 2 by H_I brings these values at large depths into the range of the hardness measured by spheres that was shown in Fig. 4.

A correlation of the indentation size effect determined with the two indenter geometries (spherical and pyramidal) can be determined from the geometrically necessary dislocations required by each indenter. The total length of geometrically necessary dislocation loops required by a spherical indenter is $\lambda = 2.09a^3/bR$ and the conical equivalent of a Berkovich indenter ($\tan \theta = 0.358$) requires a total length of $\lambda = 0.4a^3/bh$. Therefore, for $R = 5.2h$, the same total length of geometrically necessary dislocation loops is required, and the hardness measured by the two indenters is predicted to be the same. By definition, the same ratio ($R^* = 5.2h^*$) holds for the relation between the length scales used in the modeling of the indentation size effect by spherical and conical indenters with $\tan \theta = 0.358$. Fig. 5 shows this correlation by using the $R = 5.2h$ relation and plotting the hardness measured by a Berkovich indenter offset by 1.2 GPa to account for work hardening. The results for the two indenter shapes agree within one standard deviation, which corroborates the proposed correlation. The above correlation procedure was also applied

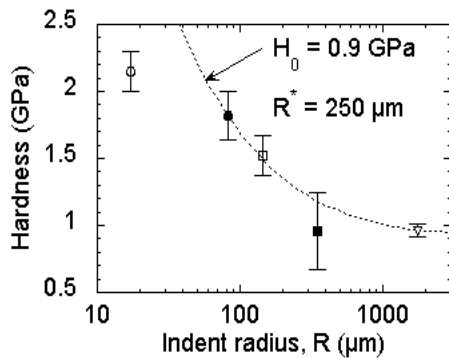


Figure 4. Indentation size effect in annealed iridium measured with spherical indenters: comparison of experiments in iridium $a/R = 0.05$ ($R = 14 \mu\text{m}$, \circ ; $R = 69 \mu\text{m}$, \bullet ; $R = 122 \mu\text{m}$, \square ; $R = 318 \mu\text{m}$, \blacksquare ; $R = 1600 \mu\text{m}$, \triangle) with the model (dotted line).

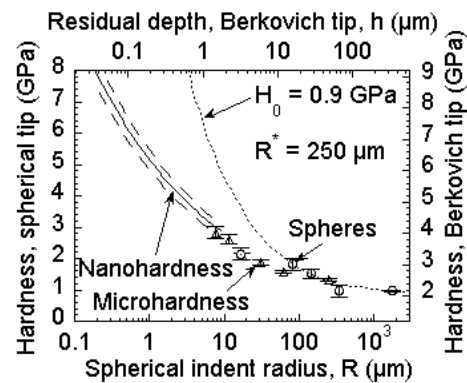


Figure 5. Correlation of the indentation size effect in annealed iridium measured with spherical indenters at $a/R = 0.05$ (\circ), with a Berkovich indenter (\triangle and solid line) and comparison of experiments with the general model (dotted line).

to the results obtained by Lim and Chaudri [9] for pyramidal and spherical indentation of oxygen free copper (OFC). The correlation was also found to accurately fit the OFC data.

CONCLUSIONS

Geometrically necessary dislocations are generated by both pyramidal and spherical indenters. Indentation with spheres of various radii was shown to determine separately the work hardening and indentation size effects. For spherical indenters, the indentation size effect is related to the radius of the sphere, while the effect of work hardening scales with the contact radius in a manner similar to the macroscopic case (see [12]).

By reexamining the geometrical necessary dislocation model [5, 7], a decoupling of work hardening and indentation size effects was found. In order to correlate the indentation size effects that are exhibited by pyramidal and spherical indenters, the increase in hardness due to work hardening that occurs during indentation can be added separately as shown in Eq. (5). After accounting for the effect of work hardening, the model predicts a correlation between the indentation size effects measured by pyramidal and spherical indenters. This correlation was verified experimentally.

ACKNOWLEDGEMENT

Research was funded by the Office of Space Power Systems and the Microscopy and Microanalytical Science Task. Research at the Oak Ridge National Laboratory SHaRE Collaborative Research Center was sponsored by the Division of Materials Sciences and Engineering, U. S. Department of Energy, under contract DE-AC05-00OR22725 with UT-Battelle, LLC. JGS gratefully acknowledges additional funding from a Director's Fellowship at Los Alamos National Laboratory.

REFERENCES

1. B. W. Mott, *Micro-indentation Hardness Testing*. (Butterworths, 1956) pp. 45-139.
2. N. A. Stelmashenko, M. G. Walls, L. M Brown and Y. V. Milman, *Acta Metall. Mater.* **41**, 2855 (1993).
3. M. S. De Guzman, G. Neubauer, P. Flinn and W. D. Nix, *Mater. Res. Soc. Symp. Proc.* **308**, 613 (1993).
4. Q. Ma and D. R. Clark. *J. Mater. Res.* **10**, 853 (1995).
5. M. F. Ashby, "The deformation of plastically non-homogenous alloys," *Strengthening Methods in Crystals*, ed. A Kelly and R. B. Nicholson, (Applied Science Publishers, Ltd., 1971) pp. 137-192.
6. J. F. Nye, *Acta Metall.* **1**, 153 (1953).
7. W. D. Nix and H. Gao, *J. Mech. Phys. Solids.* **46**, 411 (1998).
8. W. J. Poole, M. F. Ashby and N. A. Fleck, *Scripta Mater.* **34**, 559 (1996).
9. Y. Y. Lim and M. M Chaudhri., *Phil. Mag A.* **79**, 2979 (1999).
10. J. G. Swadener, E. P. George and G. M. Pharr, *J. Mech. Phys. Solids* **50**, (2002) (in press).
11. A. Arsenlis and D. M. Parks, *Acta Mater.* **47**, 1597 (1999).
12. K. L. Johnson, *J. Mech. Phys. Solids* **18**, 115 (1970).
13. W. C. Oliver and G. M. Pharr, *J. Mater. Res.* **7**, 1564 (1992).
14. J. S. Field and M. V. Swain, *J. Mater. Res.* **8**, 297 (1993).
15. H. Wiedersich, *J. Metals.* **16**, 425 (1964).